



Physical Properties of Local Wave Field Synthesis using Circular Loudspeaker Arrays

Fiete Winter and Sascha Spors

Institute of Communications Engineering, University of Rostock, R.-Wagner-Str. 31 (H8), 18119 Rostock, Germany

Summary

The reproduction accuracy of sound field synthesis techniques, like e.g. Wave Field Synthesis (WFS) or near field compensated Higher-Order Ambisonics, is limited due to practical aspects. For the audible frequency range the desired sound field can not be synthesized aliasing-free over an extended listening area, which is surrounded by a discrete ensemble of individually driven loudspeakers. However, it is suitable for certain applications to increase reproduction accuracy inside a smaller (local) listening region while stronger artifacts outside are permitted. A local Wave Field Synthesis method utilizes focused sources as a distribution of virtual loudspeakers which are placed more densely around the local listening area. These virtual loudspeakers are then driven by conventional WFS techniques. This paper establishes an analytical framework to analyze the physical properties of local WFS for circular loudspeaker arrays.

PACS no. 43.60.+d, 43.20.+g

1. Introduction

Wave Field Synthesis (WFS) and Higher-Order Ambisonics (HOA) are two well known examples of Sound Field Synthesis (SFS) techniques. They synthesize a desired acoustic scenario within an extended listening area. In theory, WFS uses a continuous distribution of acoustic sources in order to reproduce a virtual wave field. A limited number (up to hundreds) of individually driven loudspeakers placed at discrete positions around the listening area realizes this distribution in practical implementations. Spatial aliasing artifacts occur due to the finite spatial resolution of this discretization. This limits the synthesis' accuracy especially for higher frequencies. An accurate synthesis within the extended area is not possible with current WFS setups for the full audible frequency range up to 20 kHz.

For application scenarios, where the listeners' position is further restricted to a smaller region of interest, local sound field synthesis (LSFS) techniques are useful. They aim at a more accurate synthesis within a (local) area which is smaller than the entire area surrounded by the loudspeaker array. This accuracy improvement comes at the cost of stronger artifacts outside the local listening area. Among other approaches [1, 2, 3] for LSFS, a technique [4] has been proposed

which utilizes focused sources as virtual loudspeakers surrounding the local listening area. Analogue to conventional SFS these virtual loudspeakers are driven by a suitable SFS technique in order to reproduce the desired wave field within the local listening area. The SFS driven focused sources are then realized by the real loudspeaker setup. It has been shown in [4], that Wave Field Synthesis is a computationally efficient tool for implementing this LSFS technique.

This paper analyzes the LWFS approach with respect to physical properties for circular loudspeaker arrays. It focuses on the artifacts introduced by spatial sampling of the real and the virtual loudspeaker distributions. First, a short overview on the basic theory of WFS and focused sources for arbitrary array geometries is given in Sec. 2. An analytical framework based on this theory is established for LWFS. Secondly, the effects of spatial sampling are investigated by using spatio-spectral representations of the involved functions.

2. Basic Theory

2.1. Wave Field Synthesis

WFS is based on the Helmholtz Integral Equation (HIE) [5], which states the solution of the homogenous wave equation for a bounded region V_0 with respect to inhomogeneous boundary conditions imposed on ∂V_0 . A loudspeaker setup, which is placed on the boundary ∂V_0 , can be regarded as an inhomogeneous boundary

(c) European Acoustics Association

condition.

For the application of sound field synthesis it is desired to reproduce the sound field $S(\mathbf{x})$ of a virtual source situated outside the listening area V_0 (see Fig. 1). The HIE states that a distribution of secondary monopole and dipole sources on the boundary ∂V_0 has to be respectively driven by the directional gradient and pressure of the sound field of the virtual source in order to achieve reproduction inside V_0 . In this case, the sound field $P(\mathbf{x})$ inside the listening area coincides with the desired sound field $S(\mathbf{x})$. While the theory of WFS states the exact solution of the HIE for infinite planar secondary source distributions, it introduces a number of reasonable approximations to circumvent the necessity of secondary dipole sources for arbitrarily shaped boundaries. The synthesized sound field is given by

$$P(\mathbf{x}) = \oint_{\partial V_0} D(\mathbf{x}_0) G_0(\mathbf{x} - \mathbf{x}_0) dA_0, \quad (1)$$

where a position on the boundary ∂V_0 is denoted by $\mathbf{x}_0 \in \partial V_0$. The dependency on the angular frequency $\omega = 2\pi f$ is omitted in nomenclature for the whole paper. The free-field Green's function $G_0(\mathbf{x} - \mathbf{x}_0)$ characterizes the sound field emitted by a secondary spherical monopole source located at \mathbf{x}_0 . $D(\mathbf{x}_0)$ describes the driving function for the secondary sources and dA_0 a suitably chosen boundary element for integration. The WFS driving function is given as

$$D(\mathbf{x}_0) = -2 a(\mathbf{x}_0) \frac{\partial}{\partial \mathbf{n}_0} S(\mathbf{x}), \quad (2)$$

where the directional gradient $\frac{\partial}{\partial \mathbf{n}_0}$ is defined as scalar product of the boundary's inward normal vector \mathbf{n}_0 and the gradient $\nabla S(\mathbf{x})$ evaluated at $\mathbf{x} = \mathbf{x}_0$. The secondary source selection criterion $a(\mathbf{x}_0)$ ensures that only those secondary sources are active where the propagation direction of the virtual source $S(\mathbf{x})$ at the position \mathbf{x}_0 has a positive component in direction of the normal vector \mathbf{n}_0 .

2.2. Local Wave Field Synthesis

The basic concept of LWFS is to utilize a set of focused sources as a so called *virtual secondary source* distribution, which has to be driven like a real loudspeaker setup. The virtual secondary sources are distributed on the boundary ∂V_l of the local listening area $V_l \subset V_0$ (see Fig. 2). The driving signal for the virtual secondary sources is derived by migrating the equations (1) and (2) of the WFS approach (see Sec. 2.1) to the geometry of the local listening area. This domain denoted by the index "l" is referred as the *local domain*, while the *loudspeaker domain* (index 0) describes the physically existing secondary source geometry. The driving signal then reads

$$D_l(\mathbf{x}_l) = -2 a_l(\mathbf{x}_l) \frac{\partial}{\partial \mathbf{n}_l} S(\mathbf{x}), \quad (3)$$

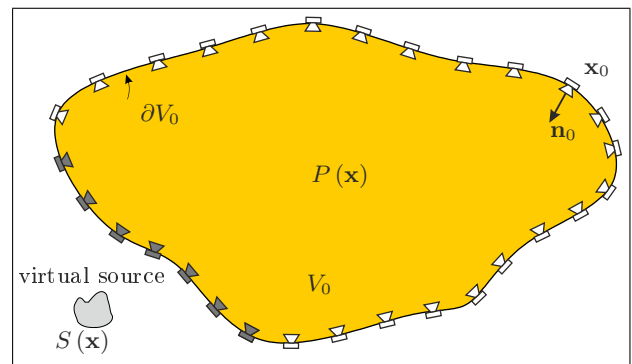


Figure 1: The desired sound field $S(\mathbf{x})$ can only be reproduced correctly inside the listening area V_0 (yellow shade). The active (dark shaded) loudspeakers are selected via the secondary source selection criterion $a(\mathbf{x}_0)$.

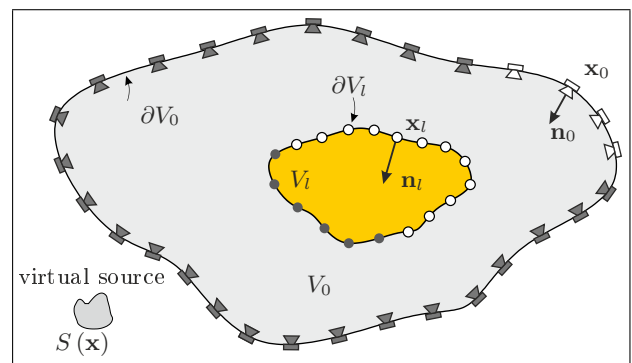


Figure 2: In Local Wave Field Synthesis the desired sound field $S(\mathbf{x})$ is only reproduced inside the local listening area V_l (yellow shade) with the virtual secondary source distribution (dots) on its boundary ∂V_l . Active (virtual) secondary sources are shaded dark.

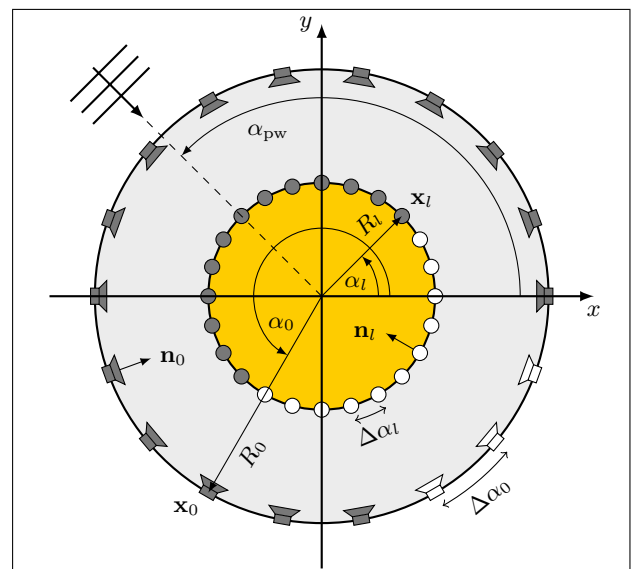


Figure 3: Concentric, circular loudspeaker for LWFS. The symbol in the upper left corner sketches a plane wave arriving from at the angle α_{pw} as the desired sound field.

Table I: The left column lists functions involved in the circular reproduction scenario described in Sec. 3. The ν th-order Hankel functions of first and second kind [6, 8.405] are respectively denoted by $H_\nu^{(1)}(\cdot)$ and $H_\nu^{(2)}(\cdot)$. The rectangular function $\text{rect}(x)$ [7, p. 201-204] equals unity for $|x| \leq 1/2$ and zero otherwise. The auxiliary variable $\alpha_R = \arccos\left(\frac{R_l}{R_0}\right)$ is introduced for ease of illustration. The coefficients of the respective circular Fourier series are given in the right column. The cardinal sine function is defined as $\text{sinc}(x) := \sin(x)/x$.

$F(\mathbf{x}) = \sum_{\mu=-\infty}^{\infty} \mathring{F}(\nu, r) e^{j\nu\alpha}$	$\mathring{F}(\nu, r) = \frac{1}{2\pi} \int_{-\pi}^{\pi} F(\mathbf{x}) e^{-j\nu\alpha} d\alpha \text{ [5, (1.25)]}$
$G_0(\mathbf{x} - \mathbf{x}_0) = -\frac{j}{4} H_0^{(2)}\left(\frac{\omega}{c} \mathbf{x} - \mathbf{x}_0 \right) \text{ [5, (8.51)]}$	$\mathring{G}_0(\nu, r) = -\frac{j}{4} J_\nu\left(\frac{\omega}{c} R_0\right) H_\nu^{(2)}\left(\frac{\omega}{c} r\right) e^{-j\nu\alpha_0} \text{ [5, (8.53)]}$
$a_{\text{fs}}(\mathbf{x}_0 - \mathbf{x}_l) = \text{rect}\left(\frac{\alpha_0 - \alpha_l}{2\alpha_R}\right)$	$\mathring{a}_{\text{fs}}(\nu) = \frac{\alpha_R}{\pi} \text{sinc}(\nu\alpha_R) e^{-j\nu\alpha_l}$
$\frac{\partial}{\partial R_0} G_0^*(\mathbf{x}_0 - \mathbf{x}_l) = \frac{j}{4} \frac{\partial}{\partial R_0} H_0^{(1)}\left(\frac{\omega}{c} \mathbf{x}_0 - \mathbf{x}_l \right) \text{ [8, (4)]}$	$\mathring{G}_0^{*'}(\nu) = \frac{j}{4} \frac{\omega}{c} J_\nu\left(\frac{\omega}{c} R_l\right) H_\nu^{(1)'}\left(\frac{\omega}{c} R_0\right) e^{-j\nu\alpha_l}$
$a_l(\mathbf{x}_l) = \text{rect}\left(\frac{\alpha_l - \alpha_{\text{pw}}}{\pi}\right) \text{ [9, (14)]}$	$\mathring{a}_l(\nu) = \frac{1}{2} \text{sinc}\left(\nu\frac{\pi}{2}\right) e^{-j\nu\alpha_{\text{pw}}}$
$\frac{\partial}{\partial R_l} S(\mathbf{x}_l) = \frac{\partial}{\partial R_l} e^{j\frac{\omega}{c} R_l \cos(\alpha_l - \alpha_{\text{pw}})} \text{ [9, (14)]}$	$\mathring{S}'(\nu) = j^\nu \frac{\omega}{c} J_\nu'\left(\frac{\omega}{c} R_l\right) e^{-j\nu\alpha_{\text{pw}}} \text{ [6, (8.511-4)]}$

while the reproduced local sound field is given as

$$P(\mathbf{x}) = \oint_{\partial V_l} D_l(\mathbf{x}_l) G_0(\mathbf{x} - \mathbf{x}_l) dA_l \quad (4)$$

for $\mathbf{x}_l \in \partial V_l$. The principle of acoustic focusing by time reversal/phase conjugation [10] allows for the realization of the free field Green's function $G_0(\mathbf{x} - \mathbf{x}_l)$ as a focused source. The reproduced sound field

$$G_0(\mathbf{x} - \mathbf{x}_l) \approx \oint_{\partial V_0} D_{\text{fs}}(\mathbf{x}_0 - \mathbf{x}_l) G_0(\mathbf{x} - \mathbf{x}_0) dA_0. \quad (5)$$

creates the impression of a monopole source at the *focus point* \mathbf{x}_l using the secondary sources located at $\mathbf{x}_0 \in \partial V_0$. The according driving function for the secondary sources is given as

$$D_{\text{fs}}(\mathbf{x}_0 - \mathbf{x}_l) = -2 a_{\text{fs}}(\mathbf{x}_0 - \mathbf{x}_l) \frac{\partial}{\partial \mathbf{n}_0} G_0^*(\mathbf{x} - \mathbf{x}_l), \quad (6)$$

where $G_0^*(\mathbf{x} - \mathbf{x}_l)$ symbolizes the conjugate complex (time reversed) free field Green's function. The secondary source selection criteria for a focused source located at \mathbf{x}_l is given as

$$a_{\text{fs}}(\mathbf{x}_0 - \mathbf{x}_l) = \begin{cases} 1 & , \text{ if } \mathbf{n}_l^T(\mathbf{x}_0 - \mathbf{x}_l) < 0 \\ 0 & , \text{ otherwise.} \end{cases} \quad (7)$$

After inserting (5) into (4) and rearranging the integrals' order the reproduced sound field is expressed by

$$P(\mathbf{x}) = \oint_{\partial V_0} D_0(\mathbf{x}_0) G_0(\mathbf{x} - \mathbf{x}_0) dA_0, \quad (8)$$

while the LWFS driving function for the secondary sources is given as

$$D_0(\mathbf{x}_0) = \oint_{\partial V_l} D_l(\mathbf{x}_l) D_{\text{fs}}(\mathbf{x}_0 - \mathbf{x}_l) dA_l. \quad (9)$$

3. Circular Loudspeaker Array

Typical implementations of WFS systems are restricted to the reproduction in the horizontal plane [4]. Modeling each loudspeaker as a monopole point source is referred to as 2.5D WFS. The following calculus is however simplified to a two-dimensional scenario utilizing secondary line sources. The effects of spatial aliasing on 2.5D setups can be inferred from the 2D case [11].

An exemplary situation for a circular loudspeaker array is illustrated in Fig. 3. All coordinates are defined within a polar coordinate system with the azimuth angle α and the radial distance r , e.g. $\mathbf{x} = [\alpha \ r]^T$. The center of the circular loudspeaker array is located at the origin of the coordinate system and its radius is denoted by R_0 . The virtual secondary source distribution is placed concentric to the loudspeakers with the radius R_l . In this paper we investigate physical properties of LWFS with respect to a virtual plane wave

$$S(\mathbf{x}) = e^{j\frac{\omega}{c} r \cos(\alpha - \alpha_{\text{pw}})}, \quad (10)$$

emerging from an angle α_{pw} as the desired sound field. The speed of sound is denoted by c . For the given geometry, the reproduced wave field (8) specializes to

$$P(\mathbf{x}) = \int_0^{2\pi} D_0(\mathbf{x}_0) G_0(\mathbf{x} - \mathbf{x}_0) R_0 d\alpha_0, \quad (11)$$

where $\mathbf{x} = [\alpha, r]^T$ with $r < R_l$ and $\mathbf{x}_0 = [\alpha_0, R_0]^T$. The two-dimensional free-field Green's function $G_0(\mathbf{x} - \mathbf{x}_0)$ (see Tab. I) describes the wave field of the loudspeakers for two-dimensional reproduction. The secondary sources' driving function (9) is given by the spatial convolution integral

$$D_0(\mathbf{x}_0) = \int_0^{2\pi} D_l(\mathbf{x}_l) D_{\text{fs}}(\mathbf{x}_0 - \mathbf{x}_l) R_l d\alpha_l, \quad (12)$$

where $\mathbf{x}_l = [\alpha_l, R_l]^T$ with $R_l < R_0$. The concentric circular setup simplifies the directional gradients $\frac{\partial}{\partial \mathbf{n}_0}$

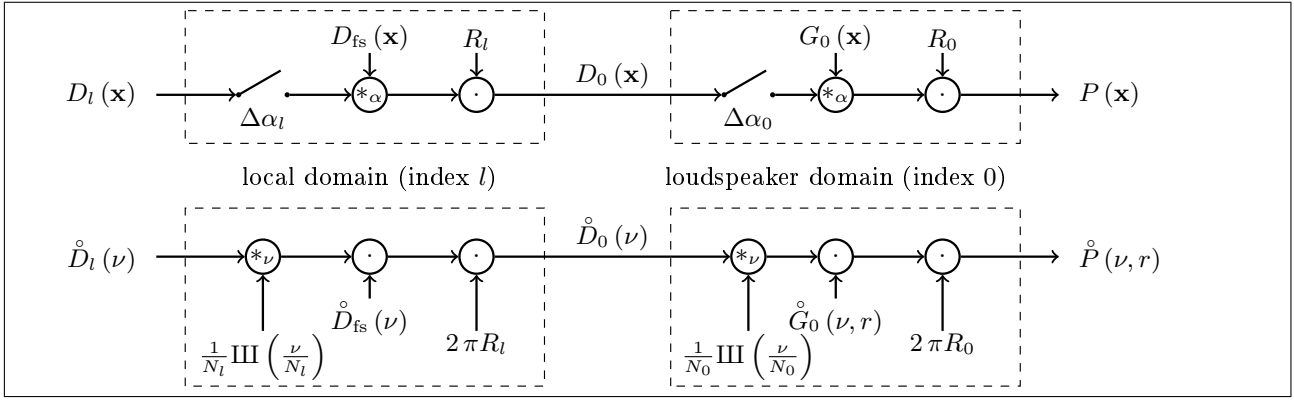


Figure 4: The upper part of the block diagram illustrates the eqs. (11) and (12). The effects of spatial sampling ($\Delta\alpha_l, \Delta\alpha_0$) are highlighted in Sec. 3.2. The spatial Fourier transform of each system component with respect to the α -coordinate is depicted in the lower part of the figure. The symbol $*$ denotes a convolution with respect to the specified variable.

and $\frac{\partial}{\partial \mathbf{n}_l}$ to the partial derivative $-\frac{\partial}{\partial r}$, evaluated at the respective radii R_0 and R_l . Hence, the driving functions involved in the right-hand side of (12) are given as

$$D_{fs}(\mathbf{x}_0 - \mathbf{x}_l) = 2 a_{fs}(\mathbf{x}_0 - \mathbf{x}_l) \frac{\partial}{\partial R_0} G_0^*(\mathbf{x}_0 - \mathbf{x}_l), \quad (13)$$

and

$$D_l(\mathbf{x}_l) = 2 a_l(\mathbf{x}_l) \frac{\partial}{\partial R_l} S(\mathbf{x}_l) \quad (14)$$

by accordingly migrating (6) and (3). The left column of Table I lists all involved functions.

3.1. Spatio-temporal Frequency Representation

The reproduced sound field is given, accordingly to eq. (11) and (12), as two cyclic convolutions along the angular coordinate α . This is illustrated by a block diagram (see Fig. 4). The 2π -periodicity of the involved functions allows for computation of the respective angular Fourier series, which are listed in the right column of Tab. I. Applying the convolution [5, (1.28)] and the multiplication [12, (D.3)] theorems of the Fourier series yields the spectrum of the reproduced sound field

$$\hat{P}(\nu, r) = 2\pi R_0 \hat{D}_0(\nu) \hat{G}_0(\nu, r) \quad (15)$$

with the spectrum of the secondary sources' driving function

$$\hat{D}_0(\nu) = \underbrace{2 \hat{a}_{fs}(\nu) *_{\nu} \hat{G}_0^{*l}(\nu)}_{\hat{D}_{fs}(\nu)} \underbrace{\left(2 \hat{a}_l(\nu) *_{\nu} \hat{S}'(\nu) \right)}_{\hat{D}_l(\nu)} \quad (16)$$

The driving functions and the free field Green's function are plotted in Fig. 5a-d for an exemplary reproduction setup. The energy of the LWFS driving function (Fig. 5c) is concentrated on less coefficients

compared to the traditional WFS driving function $\hat{D}_{WFS}(\nu)$ (Fig. 5e). Kennedy et al. [13] proved that the number of non-zero Fourier coefficients M needed for the reproduction of a monochromatic soundfield inside a circular area is depending on its radius. For given upper bound ϵ of the mean square error between the reproduced and the desired soundfield [13, (36)]

$$M(\omega) = \left\lceil \frac{eR_{\{0,l\}}}{2c} \omega \right\rceil + \left\lceil \frac{1}{2} \ln \left(\frac{0.0093}{\epsilon} \right) \right\rceil, \quad (17)$$

where $\lceil \cdot \rceil$ denotes the ceiling operator. The white lines in Fig. 5c and Fig. 5e show $M(\omega)$ for a tolerance of $\epsilon = 10^{-5}$. The radii of listening areas R_l and R_0 have been inserted into (17) for the respective reproduction method. A comparison of the bounds with the respective spectra reveals, that the energy concentration in LWFS is a result of spatial bandlimitation, i.e. a smaller listening area. This has further impact on the aliasing properties of LWFS, which will be discussed in the next section.

3.2. Spatial Sampling

For practical reproduction setups circular loudspeaker arrays consist of a finite number N_0 of loudspeakers (see loudspeaker symbols in Fig. 3). Also the number of virtual secondary sources N_l has to be finite due to limited computational resources (see bullets in Fig. 3). It has already been outlined by Start [15, p. 73-79] that the discretization of the (virtual) secondary source distribution can be interpreted as a spatial sampling and interpolation process. As illustrated in Fig. 4, this process is divided into two sub-steps for the local and the loudspeaker domain, both applying sampling and interpolation. The equidistant discretization of both distributions is modelled by multiplying the respective driving function with a Dirac

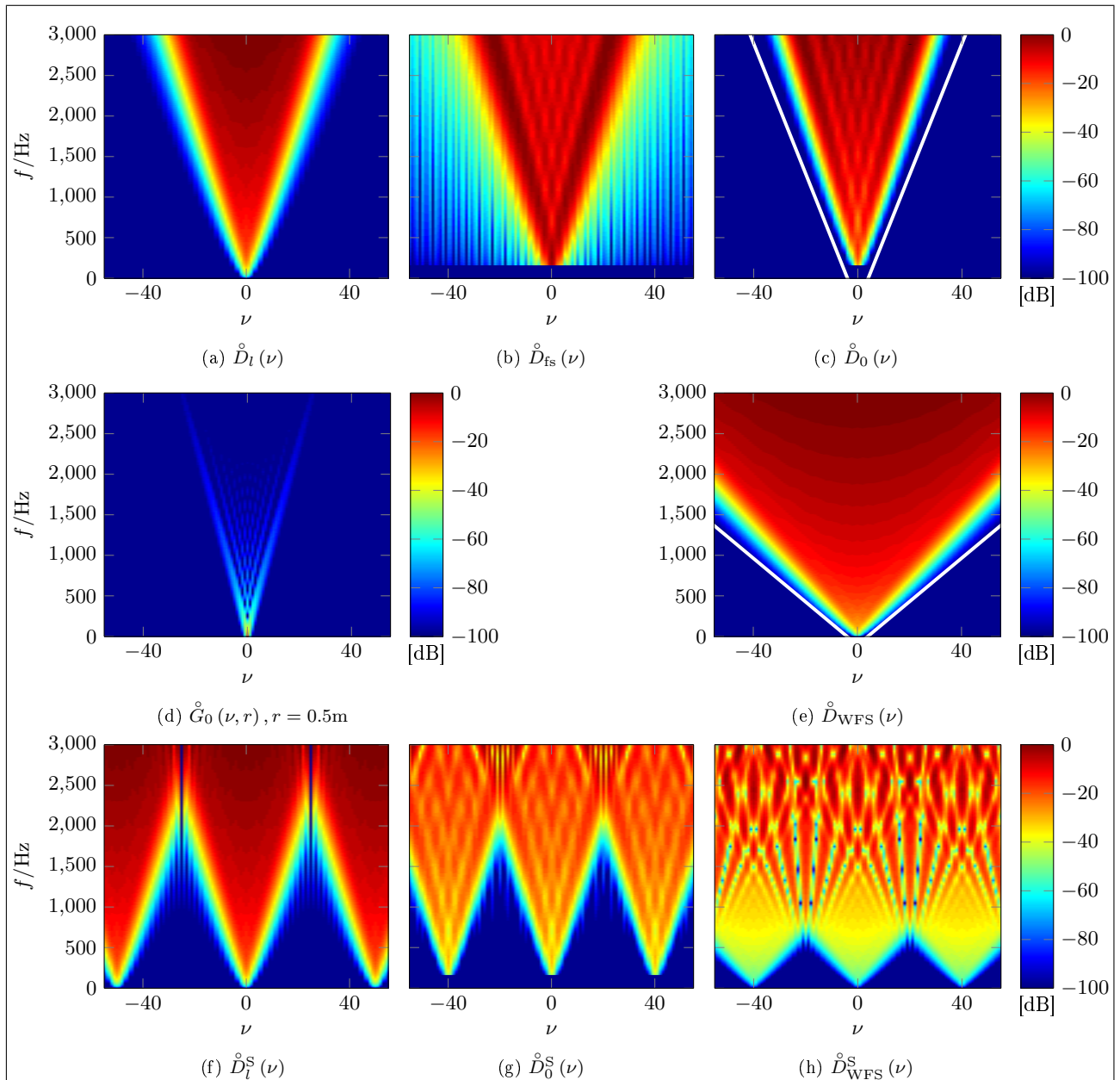


Figure 5: The continuous spectra involved in eqs. are shown in Figs. a-d. For comparison purposes, the spectra of the traditional WFS driving function is plotted in Fig. e. The figures f-h depict the discretized spectra discussed in section 3.2. For all plots the following parameters were used: $R_0 = 1.5\text{m}$, $R_l = 0.5\text{m}$, $N_0 = 40$, $N_l = 50$.

comb

$$\text{III} \left(\frac{\alpha}{\Delta\alpha_{\{0,l\}}} \right) := \Delta\alpha_{\{0,l\}} \sum_{\eta=-\infty}^{\infty} \delta(\alpha - \eta\Delta\alpha_{\{0,l\}}), \quad (18)$$

in the spatial domain, where $\Delta\alpha_{\{0,l\}} = 2\pi/N_{\{0,l\}}$ denotes the sampling distance. The wildcard symbol $\{0,l\}$ is replaced by either 0 or l for the respective domain. The angular Fourier spectra of the discrete driving signals [9, (15)]

$$\mathring{D}_{\{0,l\}}^S(\nu) = \sum_{\eta=-\infty}^{\infty} \mathring{D}_{\{0,l\}}(\nu - \eta N_{\{0,l\}}) \quad (19)$$

are given as a superposition of the shifted continuous spectra $\mathring{D}_{\{0,l\}}(\nu - \eta N_{\{0,l\}})$. After each sampling step the spatial interpolation filters $\mathring{D}_{\text{fs}}(\nu)$ and $\mathring{G}_0(\nu, r)$ are applied, respectively. Introducing the sampled driving functions into eq. (16) and (15) results in the spectrum $\mathring{P}^S(\nu, r)$ of the wave field reproduced by a spatially discrete (virtual) secondary source distribution.

Figures 5f and 5g illustrate the discrete spectra of the driving functions for the local and the loudspeaker domain, respectively. Aliasing contributions can be recognized by the overlapping parts of the continuous

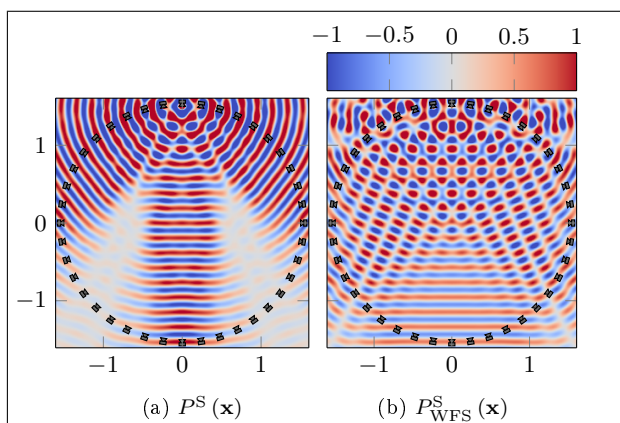


Figure 6: The diagrams show the real part of the reproduced sound field for LWFS and traditional WFS with the same parameters as in Fig. 5. The desired sound field is a plane wave arriving from $\alpha_{pw} = 90^\circ$. The sound fields are normalized to their absolute value at $[0, 0]^T$ m. The loudspeakers' positions are depicted by the symbols. The plots have been generated with the Sound Field Synthesis Toolbox [14].

spectra (centered around $\nu = 0$) and the spectral repetitions. Note, that due to the concatenation of both domains, the resulting wave field $\hat{P}^S(\nu, r)$ might contain aliasing from both domains. However, the number of virtual secondary sources N_l is not constrained by the practical loudspeaker setup but rather a matter of computational effort. The aliasing effects in the local domain can therefore be decreased by realizing more focused sources. In the loudspeaker domain the spatial bandlimitation of the continuous LWFS driving function $\hat{D}_0(\nu)$ leads to reduction of aliasing compared to the traditional WFS driving function (see Fig. 5h). This can also be recognized when comparing the reproduced sound fields (see Fig. 6).

4. Conclusion

This paper presented a detailed analysis of the physical properties of two-dimensional Local Wave Field Synthesis using focused line sources as virtual secondary sources. For discrete, circular secondary line source distributions, aliasing properties have been analysed. These state a trade-off between an artifact-free reproduction up to a certain temporal frequency and the size of the listening area for which the reproduction can be achieved. In principle, these derivations will also hold for the more practical case of 2.5D reproduction using secondary point sources.

Listening experiments [16] have indicated that timbral perception of WFS is connected to spatial aliasing caused by the limited number of loudspeakers. Although the results of this paper might allow for the conclusion that the LWFS approach has favourable colouration properties than traditional WFS, subjec-

tive experiments have to be made in order to give a well-grounded judgement for this.

Acknowledgement

This research has been supported by EU FET grant Two!EARS, ICT-618075.

References

- [1] E. Corteel, C. Kuhn-Rahloff, and R. Pellegrini, "Wave Field Synthesis Rendering with Increased Aliasing Frequency," in *Proc. of 124th Aud. Eng. Soc. Conv.*, (Amsterdam, The Netherlands), 2008.
- [2] J. Hannemann and K. D. Donohue, "Virtual Sound Source Rendering Using a Multipole-Expansion and Method-of-Moments Approach," *J. Aud. Eng. Soc.*, vol. 56, no. 6, pp. 473–481, 2008.
- [3] Y. J. Wu and T. D. Abhayapala, "Spatial multizone soundfield reproduction," in *IEEE International Conference on Acoustics, Speech, and Signal Processing (ICASSP)*, (Taipei, Taiwan), pp. 93–96, Apr. 2009.
- [4] S. Spors and J. Ahrens, "Local Sound Field Synthesis by Virtual Secondary Sources," in *Proc. of 40th Intl. Aud. Eng. Soc. Conf. on Spatial Audio*, (Tokyo, Japan), 2010.
- [5] E. G. Williams, *Fourier Acoustics: Sound Radiation and Nearfield Acoustical Holography*. London: Academic Press, 1999.
- [6] I. Gradshteyn and I. Ryzhik, *Table of integrals, series, and products*. Academic Press, 7th ed., 2007.
- [7] B. Girod, A. Stenger, and R. Rabenstein, *Signals and Systems*. Wiley, 2001.
- [8] S. Spors and J. Ahrens, "Spatial Sampling Artifacts of Focused Sources in Wave Field Synthesis," in *NAG-DAGA International Conference on Acoustics*, (Rotterdam, The Netherlands), 2009.
- [9] S. Spors and J. Ahrens, "A comparison of wave field synthesis and higher-order Ambisonics with respect to physical properties and spatial sampling," in *Proc. of 125th Aud. Eng. Soc. Conv.*, (San Francisco, USA), 2008.
- [10] D. de Vries and A. J. Berkhout, "Wave theoretical approach to acoustic focusing," *J. Acoust. Soc. Am.*, vol. 70, no. 3, 1981.
- [11] S. Spors and J. Ahrens, "Spatial Sampling Artifacts of Wave Field Synthesis for the Reproduction of Virtual Point Sources," in *Proc. of 126th Aud. Eng. Soc. Conv.*, (Munich, Germany), 2009.
- [12] J. Ahrens, *Analytic Methods of Sound Field Synthesis*. T-Labs Series in Telecommunication Services, Berlin Heidelberg: Springer-Verlag, 2012.
- [13] R. Kennedy, P. Sadeghi, T. Abhayapala, and H. M. Jones, "Intrinsic limits of dimensionality and richness in random multipath fields," *Signal Processing, IEEE Transactions on*, vol. 55, pp. 2542–2556, June 2007.
- [14] H. Wierstorf and S. Spors, "Sound Field Synthesis Toolbox," in *Proc. of 132nd Aud. Eng. Soc. Conv.*, (Budapest, Hungary), Apr. 2012.
- [15] E. W. Start, *Direct Sound Enhancement by Wave Field Synthesis*. PhD thesis, Delft University of Technology, 1997.
- [16] H. Wierstorf, C. Hohnerlein, S. Spors, and A. Raake, "Coloration in Wave Field Synthesis," in *Proc. of 55th Intl. Aud. Eng. Soc. Conf. on Spatial Audio*, (Helsinki, Finland), Aug. 2014.